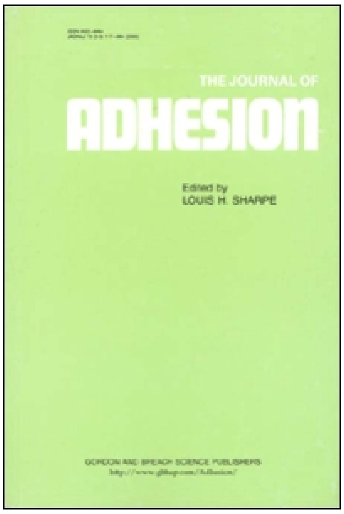

The Journal of Adhesion
Publication details, including instructions for authors and subscription information:
http://www.informaworld.com/smpp/title~content=t713453635

The Effect of Stress Whitening on Moisture Diffusion in Thermosetting Polymers

Erol Sancaktar[a]; David R. Baechtle[a]
[a] Department of Mechanical and Aeronautical Engineering, Clarkson University, Potsdam, New York, U.S.A.

To cite this Article Sancaktar, Erol and Baechtle, David R.(1993) 'The Effect of Stress Whitening on Moisture Diffusion in Thermosetting Polymers', The Journal of Adhesion, 42: 1, 65 — 85
To link to this Article: DOI: 10.1080/00218469308026571
URL: http://dx.doi.org/10.1080/00218469308026571

J. Adhesion, 1993, Vol. 42, pp. 65–85
Reprints available directly from the publisher
Photocopying permitted by license only

Printed in the United States of America.

The Effect of Stress Whitening on Moisture Diffusion in Thermosetting Polymers

EROL SANCAKTAR and DAVID R. BAECHTLE

Department of Mechanical and Aeronautical Engineering, Clarkson University, Potsdam, New York 13699, U.S.A.

(Received November 30, 1991; in final form February 12, 1993)

The effects of stress whitening on the moisture diffusion rate and concentration in a polymer adhesive containing a secondary phase were investigated. This was accomplished by performing an absorption test on both stress whitened and virgin samples of the bulk adhesive and comparing the rate and amount of moisture diffusion in each. The presence of stress whitening in samples was not only observed visually, but also confirmed analytically using the "Bilinear RAMOD-2" equation. Experimental results reveal that visibly-present stress whitening resulting from fracture does indeed affect the rate and amount of moisture absorption in a polymer adhesive. Consequently, a diffusion model representing two different regions, stress-whitened and non-stress-whitened, is proposed for path of diffusion in polymer adhesives.

KEY WORDS moisture diffusion in adhesives; water uptake; diffusion model; stress whitening; toughened adhesives; adhesive cracks; secondary phases in polymers; bulk moduli ratio.

INTRODUCTION

Many polymers used as adhesives or as matrix materials in composites contain secondary phases for the purposes of increasing the toughness, matching the coefficient of thermal expansion to the substrate, modifying the elastic modulus, increasing the strength, improving the handling and manufacturing conditions and thickness control, etc. The secondary phase in these cases is usually a dispersed phase such as randomly dispersed particles. Of course, in long and short fiber composites the fibers themselves constitute a secondary phase. In either one of these cases loading of the polymer leads to stress concentrations at the interphase regions between the polymer matrix and the secondary phase. Such stress concentrations may result in debonding of the polymer from the secondary phase and may also lead to plastic deformation of the polymer in these regions in the form of cavitation, shear banding (to connect the cavitated regions) and microcracking. Obviously, such localized failure will lead to an increase in the free volume within the polymer structure. The presence of macroscopic discontinuities such as drilled holes, etc., facilitates this internal failure mechanism locally. Consequently, the described microscopic failure process often remains localized without causing catastrophic failure but may deteriorate the whole polymer structure by acting as a path of moisture diffusion. It should be noted that crazing is observed not only in polymers containing secondary phases but also in single-phase polymers. The presence of a secondary phase, however, is known to lower the threshold for the onset of stress whitening and, consequently, increase its intensity.

Moisture ingression can affect composite materials and adhesively-bonded joints through two mechanisms, deterioration of the adhesive bulk and deterioration of the interface due to hydrolysis (preferential replacement of adhesive bonds by hydrogen bonding to water molecules). It is well-known that the mechanical properties of polymer-based adhesives can be degraded by the absorption of moisture from humid environments. For example, Schmidt and Bell[1] report 66% and 70% reductions in tensile modulus and yield stress, respectively, for 5-mil thick Epon 1001/V115 films which absorbed 3–3.5% water by weight as a result of immersion at 134.6°F (57°C). Furthermore, on the bulk of the adhesive the effects of moisture manifest themselves in mechanical dilatation (swelling) and plasticization.

The Stress Whitening Phenomenon

During our previous investigations with Metlbond 1113 and 1113-2 rubber-toughened epoxy adhesives (with and without carrier cloth, respectively) it was observed that stress whitening takes place prior to complete failure. This observation was made with bulk tensile[2] and shear[3] and with bulk[4] and bonded[5] fracture samples. Similar observations on the same model adhesive were reported earlier by Brinson *et al.*[6] They reported that the "crazes" they observed were both normal and at various angles to the loading direction. These angles ranged from approximately 45° to 90° with respect to the loading axis. Brinson *et al.* reported that the "crazing" process they observed in Metlbond adhesives was evidence of local damage or failure mechanism which occurred well in advance of gross fracture. They also stated that the "crazed" areas of the model adhesives were not true cracks but areas of lower density.

Yee *et al.*[7,8] conducted mechanical and microscopy studies on the toughening mechanisms in rubber-modified epoxies. Through Scanning Electron Microscopy (SEM) of the whitened zone, they found that rubber particles and the matrix had cavitated and that the sizes of these cavities were larger than the diameters of the undeformed rubber particles as determined by TEM.

In elastoplastic analysis of brittle epoxy adhesives several investigators[5,9,10] used Irwin's[11] concept of a plastic deformation zone at the tip of a crack to resolve the issue of stress singularity at that location. The approximate diameter for this zone, calculated on the basis of measured Mode-I strain energy release rate (G_{IC}) and bulk tensile properties (tensile strength, Young's modulus and, Poisson's ratio), was also suggested as the optimum adhesive thickness for bonded joints.[5,9] This suggestion was offered to ensure obtaining the maximum G_{IC} value in bonded specimens as it is obtained in bulk samples.

As confirmed by visual and microscopic evidence, it is the authors' belief that such a plastic deformation zone at the tip of a crack encompasses a stress-whitened zone. An exact correlation between the plastic zone diameter and the size and shape of the stress-whitened zone is not yet available. Since Irwin's analysis is based on a small scale yielding assumption and does not describe the shape of the plastic deformation zone accurately, the presence of a circular deformation zone should be considered only hypothetical. In fact, mathematical functions describing the exact shape of crack tip plastic deformation zones for monolithic samples are available in the literature.[12,13]

During our previous bulk fracture experiments on Metlbond adhesives,[14,15] the crack tip stress whitening on the specimen surfaces perpendicular to the fracture plane was observed to occur prior to rapid crack growth. We observed that, as the load was increased, a stress-whitened zone developed at the crack tip up to a certain extent beyond which the specimen failed rapidly. The specimens which had a carrier cloth exhibited larger areas of Crack Tip Stress Whitening Zones (C.T.W.Z.). It was also observed that the specimens with higher degree of C.T.W.Z. had rougher fracture surfaces indicating a more stable crack growth while those exhibiting little or no C.T.W.Z. (low cure temperature) had very smooth fracture surfaces. The presence of voids in the highly-stressed regions of the adhesive also seemed to increase the degree of stress whitening there.

THEORETICAL CONSIDERATIONS

Water Uptake and Its Relation to Free Volume

The time change of water concentration in a three-dimensional element of (adhesive) material is described by Fick's second law:

$$\partial C/\partial t = D\{\partial^2 C/\partial x^2 + \partial^2 C/\partial y^2 + \partial^2 C/\partial z^2\} \qquad (1)$$

where C is the water concentration, D is the diffusion coefficient, t is time and, x, y, z represent space variables in an orthogonal coordinate system.

It is known that the diffusion coefficient is a function of the free volume in the material[16] and the exponential function has been used for this purpose when the material is loaded in its elastic range.[16] In such cases, the use of an exponential function coincides with the application of a probability distribution function (*i.e.* an exponential function) describing the probability for "n increments of free volume of average size V_f" accumulating into a void size, V_c, so that an equation of the form[16]

$$D = D_O \exp(A\ V_c/V_f) \qquad (2)$$

can be used. When the (toughened) adhesive material is loaded so as to stress whiten, however, a large amount of free volume is created and, consequently, the probability of water molecules reaching to and occupying free volume is increased greatly. In other words, the magnitude of the diffusion coefficient increases and the free volume created as a result of stress whitening is occupied by water within a relatively shorter time. When this process is complete, however, diffusion continues at a slower pace with the non-stress-whitened regions (which have lower probability of being reached by water) absorbing water. During this phase of water diffusion the coefficient of diffusion has a much smaller value. This is the basis of the "multi-valued" diffusion coefficient model we adopt in this paper.

The free volume, f, in polymeric materials is assumed to be affected by i) free volume dilatation, ϵ_{kk}^{f}, as created by external loads, ii) thermal expansion and iii) swelling. The individual effects due to each one of these mechanisms are assumed to be linearly additive[16] so that

$$f = f_o + \epsilon_{kk}^{f} + \alpha \Delta T + \gamma C \tag{3}$$

where α and γ are the coefficients of thermal expansion and swelling for the free volume and f_o is the free volume in the reference state.

The free volume dilatation, ϵ_{kk}^{f}, can be related to the mechanical volumetric strain, ϵ_{kk}, with the use of bulk moduli for the free volume and elastic polymer material, K_f and K, respectively:

$$\epsilon_{kk}^{f} = (K/K_f)\, \epsilon_{kk}. \tag{4}$$

Note that, in the absence of other effects, ϵ_{kk}^{f} is identical with free volume increase in the material.

By using the classical definition of volume strain, we can now write

$$f = (K/K_f)\, \epsilon_x\, [1 - 2\nu] \tag{5}$$

when swelling and thermal expansion effects are not present. In equation (5), ϵ_x is the tensile strain imposed in the "x" direction and ν is the Poisson's ratio. For a rubber-toughened, thermosetting, solid film adhesive, Brinson *et al.*[6] report that the Poisson's ratio decreased considerably once the stress whitening had occurred. This reduction depended on the rate of loading and was as much as 42% when the Poisson's ratio decreased from 0.388 to 0.226.

For the compressibility ratio, β/β_f, Ferry[17] reports values of 2 or larger. Since the compressibility is interpreted as the inverse of the bulk modulus, we expect the ratio K_f/K to be equal to 2 or larger or the ratio K/K_f of equation (5) to be 0.5 or smaller.

Multi-Valued Diffusion Coefficient: Regions of Different Densities

Broutman and Wong[18,19,20] proposed a diffusion model which assumes two different regions in the path of diffusion: 1) less dense, which will be interpreted as the stress-whitened regions for the present work and 2) dense, which will be interpreted as non-stress-whitened regions. Accordingly, the effective diffusion coefficient (D_{eff}) in the path of diffusion becomes:

$$D_{eff} = D_1 F^1 (C) + D_2 [1 - F^1 (C)] \tag{6}$$

where the coefficients D_1 and D_2 depend on the density of the regions in the absorption path with D_1 representing the less dense regions. The value of F^1 depends on the concentration of the absorbed water molecules with: $F^1 (C) \sim 1$ at low concentrations and, $F^1 (C) < 1$ at high concentrations where the contribution from the dense regions becomes significant.

Broutman and Wong originally proposed equation (6) to describe the effects of free volume distribution produced spontaneously by density fluctuations created by molecular motions.[20] We interpret the idea of density fluctuation to apply to the case of stress-whitened (less dense) *vs.* non-stress-whitened (more dense) regions based on the free volume concept.

Modeling of the Stress Whitening Phenomenon

Brinson *et al.*[6,21] reported that the most suitable model that would fit the stress-strain response of the model (Metlbond, Narmco) adhesives with prediction of the stress whitening stress level, σ^*, was a modified version of the Ramberg-Osgood equation, which they called the "Bilinear RAMOD-2" equation. The bilinear behavior was obtained when $\log(\epsilon_p)$ was plotted against $\log(\sigma_p)$. The plastic strain ϵ_p was assumed to be a function of the over-stress above the elastic limit stress, θ, and the stress levels defining the intersection point for the bilinear behavior were found to occur slightly below the stress-whitening stress values. The bilinear RAMOD-2 has the form:

$$\begin{aligned} &\epsilon=\sigma/E && 0\le\sigma\le\theta \\ &\epsilon=(\sigma/E)+K_1\ (\sigma-\theta)^{n1} && \theta\le\sigma\le\sigma^* \\ &\epsilon=(\sigma/E)+K_2\ (\sigma-\theta)^{n2} && \sigma^*\le\sigma\le\sigma_{\max} \end{aligned} \tag{7}$$

where K_1, n_1, K_2, n_2 are the material constants determined empirically from a bilinear log-log plot of ϵ_p *vs.* $(\sigma-\theta)$. In the bilinear RAMOD-2 model, σ^* is defined as the stress at the intersection of the bilinear plots of $\log(\epsilon_p)$ *versus* $\log(\sigma-\theta)$.

Renieri *et al.*[21] observed that equation (7) could fit their stress-strain results for Metlbond 1113 and 1113-2. Moreover, they realized the significance of σ^* in connection with the stress-whitening phenomenon that occurred in the tensile samples before fracture. They observed the stress-whitening stress and strain values experimentally (through visual observation). They found that σ^* and the corresponding strain values (ϵ^*), as determined from equation (7), were very close to the experimentally-observed values at stress whitening. Therefore, one may conclude that the presence of stress whitening and existence of σ^*, *i.e.* a bend in the $\log(\epsilon_p)$ *vs.* $\log(\sigma-\theta)$ data, are directly related.

Subsequent research by Sancaktar *et al.*[14,15] on the same phenomenon confirmed the findings of Brinson *et al.* which were summarized above.

The RAMOD-2 model will be used in this work to locate the stress-whitening stress and to confirm the presence of stress whitening in the samples. This is accomplished in the following manner.

The vertical axis of the RAMOD-2 plot is the $\log(\sigma-\theta)$ while the horizontal axis is the $\log(\epsilon_p)$. The data recorded during the loading of each sample, in most cases, only contains corresponding values of stress (σ) and total strain (ϵ_T). Thus, it is necessary to predetermine certain values and perform other intermediate calculations before the RAMOD-2 plots can be constructed. With the aid of a computer program which was developed, it is possible to generate the RAMOD-2 data for a given sample by predetermining the values of only two variables, *i.e.* E and θ.

For the computer program to be capable of determining the $\log(\sigma-\theta)$ value, it is necessary to predetermine the value of the elastic limit stress, θ, for each respective sample where the loading curve deviates from linearity. This is done by fitting a straight line to the initial linear portion of the loading curve (slope E) and noting the point where the loading curve begins to deviate from it (point θ).

In order to determine the $\log(\epsilon_p)$ value, it is first noted that:

$$\epsilon_p = \epsilon_T - \epsilon_e \tag{8}$$

where ϵ_e is the elastic strain:

$$\epsilon_e = \theta / E \tag{9}$$

and ϵ_T is simply the recorded strain value. The sample's elastic modulus, E, is determined by noting the slope of the straight line which had been fit to the initial linear (elastic) portion of the loading curve.

Initial application of the RAMOD-2 plots to the current model adhesive revealed that several bilinear curves, yielding different σ^* values, could be fitted to each individual plot. In order to eliminate any error which would have been caused by arbitrarily fitting a single bilinear curve to each plot, two bilinear curves were fitted to each plot. In this manner it was possible to develop a range for σ^*. From the lower curve a value for the lowest possible stress whitening stress (σ^*_L) was recorded and from the upper curve, a value for the highest possible stress whitening stress (σ^*_U) was recorded.

EXPERIMENTAL CONSIDERATIONS

The model material used was EA 9628NW, a thermosetting, modified epoxy film adhesive containing a non-woven nylon mat. This material is manufactured by Dexter Hysol, Aerospace and Industrial Products Division, Pittsburg, CA, USA.

The samples were cured in a forced air convection oven manufactured by Applied Test Systems, Inc. (Saxonburg, PA). This oven was attached to a ramp and soak controller, also manufactured by Applied Test Systems Inc. (Butler, PA). The cure schedule complied with the manufacturer's high temperature cure specifications and can be seen in Figure 1.

After curing, the samples were sanded down to a uniform thickness using a pad sander and 100, 150, 220, and 400 grit sandpaper in succession. The samples were then cut to the dimensions shown in Figure 2 with the aid of a template mounted on a routering fixture. Each sample was fixed on the template using double-backed tape and subsequently cut into the dog-bone shape using a router equipped with a tracing bit. The samples were then sanded by hand with 400 grit sandpaper to remove any flash or rough edges left by the router. The cross-sectional area of each sample was also measured at this point with any drastic deviations from the standard being alleviated by additional sanding with the 400 grit sandpaper.

Sample Loading

To date, most of the experiments which have investigated the phenomenon of stress-coupled moisture diffusion have followed experimental procedures which are

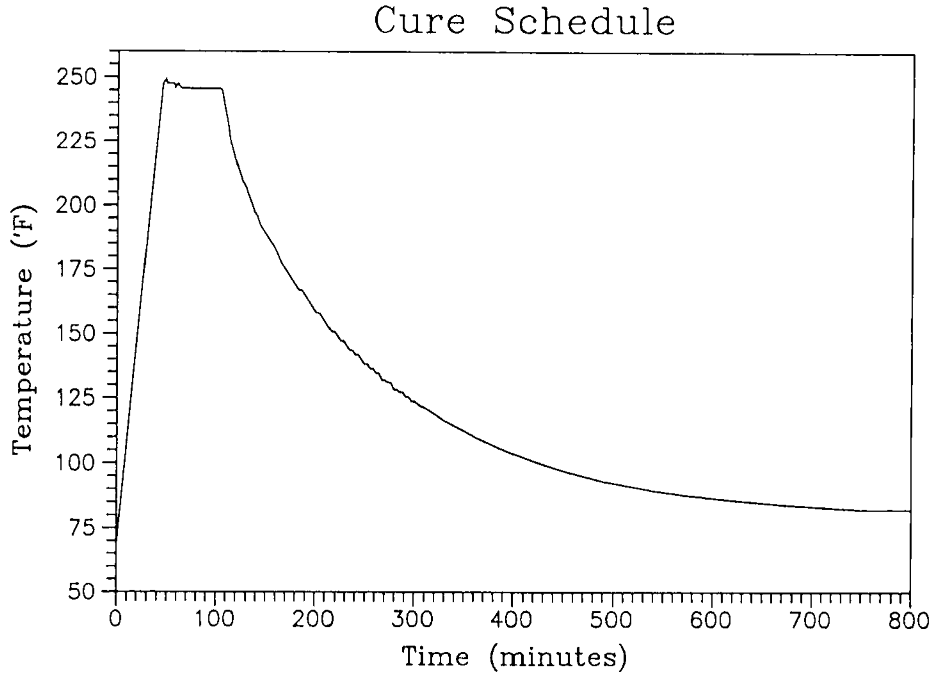

FIGURE 1 Oven temperature profile during the cure process.

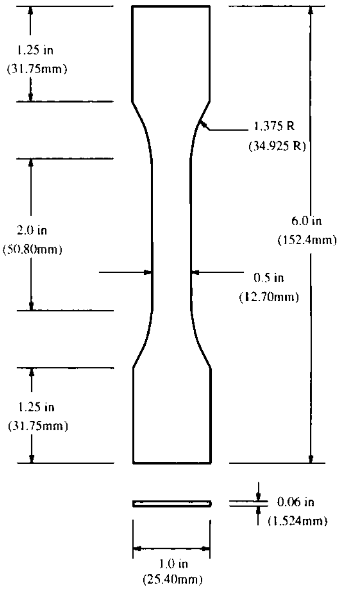

FIGURE 2 Dimensions of the samples used in experiments A and B.

quite similar: That is, the samples in these investigations were simultaneously exposed to moisture and a sustained load. In the present work, however, the samples were loaded and then immediately unloaded before being subjected to moisture. Thus, the loading history of these samples, and any damage caused by this loading, could be firmly established and quantified before moisture absorption testing. For this purpose, the samples were grouped based on the different levels of tensile stress to which they were subjected, with each group containing four samples (*i.e.* 4 groups × 4 samples = 16 samples). The samples of group 1 in each experiment were left unstressed (virgin). The samples in group 2 of each experiment were stressed just slightly beyond the elastic limit of the material but below the stress-whitening stress σ_L^*. Group 3 samples were stressed to the beginning of plastic deformation, just beyond the stress-whitening stress (*i.e.* slightly above σ_U^*). The last group of samples, group 4, were stressed all the way to failure, well beyond the stress-whitening stress level. Two groups of experiments (experiments A and B) were performed in this fashion providing data on a total of 32 samples.

All the samples were loaded by an Instron 1331 testing machine at a constant cross-head rate of 0.1 in/min (2.5 mm/min). The stress/strain data for each sample were obtained by interfacing the Instron and an extensometer mounted directly to the specimen with a Zenith Z-100 computer.

Moisture Absorption Testing

Coupons approximately one inch (25.4 mm) long were cut from the gauge-length of each stressed or unstressed specimen to be used for absorption testing. The cut edges of each of these coupons were sanded slightly with 400 grit sandpaper to remove any flash, chips, or irregularities which could have affected the subsequent weighing of each coupon.

To assure that none of the coupons contained any moisture at the start of the absorption test, all the coupons were placed in a sealed container along with a desiccate for a minimum of forty-eight hours. Upon removal from the desiccate, each coupon was weighed immediately on the Mettler PE360 DeltaRange scale, which is accurate to 0.001 grams. The weight obtained at this first weighing was taken to be the "dry" or initial weight of the coupon. After this first weighing, the coupons were placed in a sample holder and immersed in a bath of de-ionized (di) water. This water was kept at a constant temperature of 104 ± 1°F (40°C) by a model FE-2 constant temperature bath manufactured by Haake.

The coupons were periodically removed from the constant temperature bath, dried of any surface water with a paper towel and weighed on the Mettler scale. During the initial stages of the test the coupons absorbed water at a relatively fast pace and it was necessary to weigh them every few hours. However, as the experiment progressed, the coupons absorbed at a slower rate and it became necessary to weigh the coupons only once a day, or once every few days.

RESULTS AND DISCUSSION

Subsequent to loading, the stress-strain data recorded were graphically displayed for each individual sample. An example of these stress-strain diagrams is shown in Figure 3. The stress-strain diagrams for specimen groups 2B, 3B and 4B are shown collectively in Figures 4–6, respectively. The amount of irreversible (stress-whitening) strain induced in each group can be observed in these figures to approximate the amount of free volume dilatation induced. Examination of Figure 4 reveals that the group 2 specimens, on the average, did not acquire any appreciable amount of irreversible strain while the group 3 specimens had an average of (approximately) 0.006 in/in irreversible strain (Figure 5). Group 6 specimens, however, exhibit approximately an average of 0.04 in/in irreversible strain (Figure 6).

RAMOD-2 plots for the individual samples in groups 3 and 4 were then constructed in the manner described earlier. A typical example of these RAMOD-2 plots is shown in Figure 7. From the RAMOD-2 plots it was possible to determine the stress-whitening stress range corresponding to each sample.

During the stressing of the samples in group 4, the point at which stress whitening became visually apparent in each sample was recorded. The visually-observed stress-whitening stress values, σ_V^*, proved to be slightly higher than the upper limit of the stress-whitening stress range, σ_U^*.

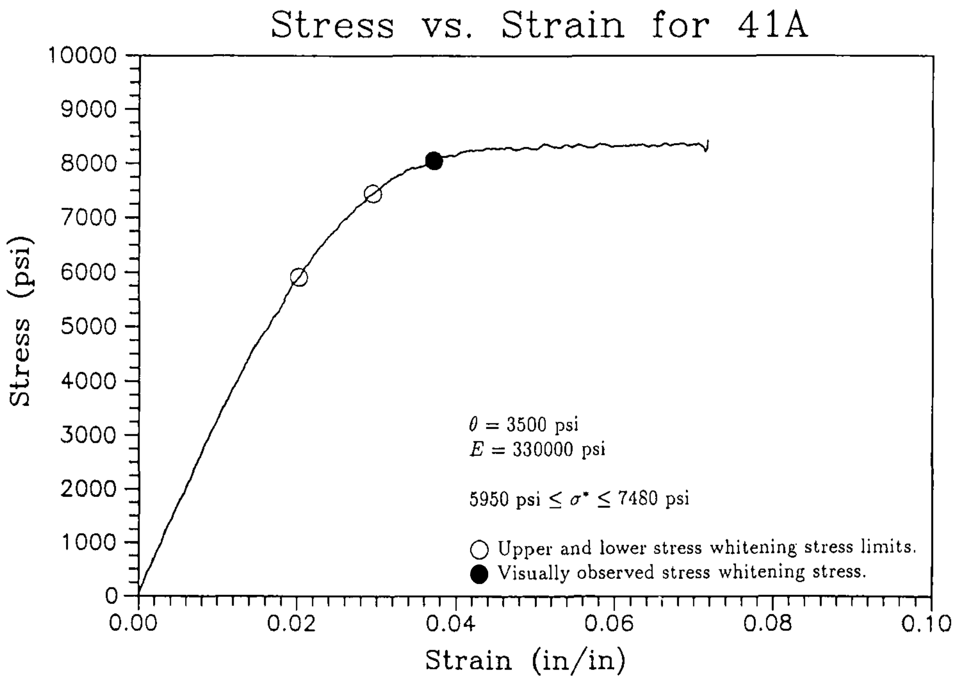

FIGURE 3 Sample stress-strain diagram illustrating upper and lower stress whitening stress limits σ_L^* and σ_U^* and the level of visually-observed stress whitening stress, σ_V^*.

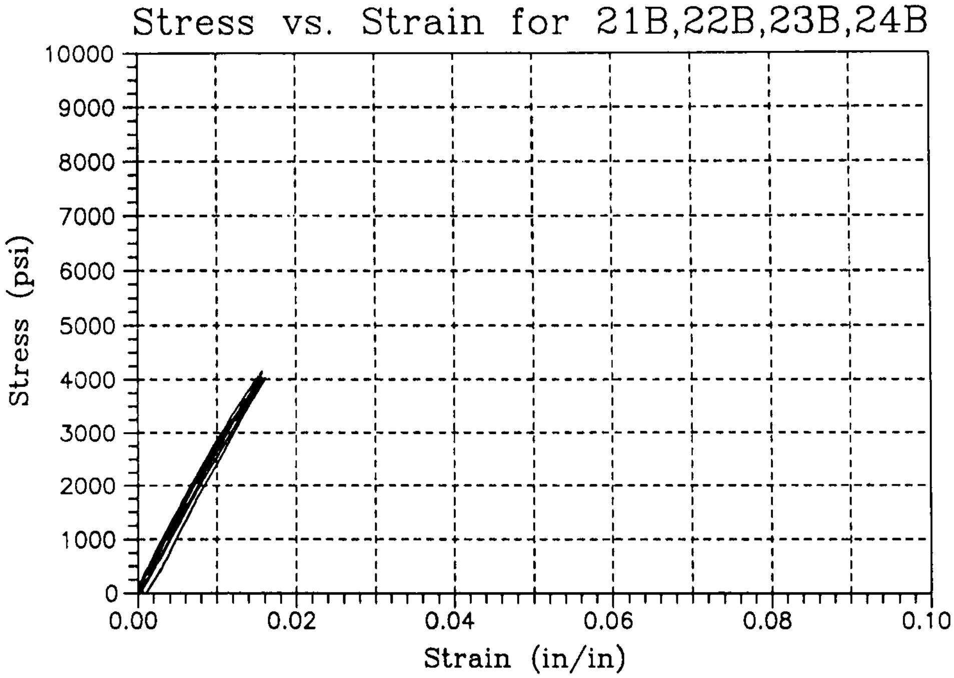

FIGURE 4 Loading/unloading diagram for experiment B, group 2 samples.

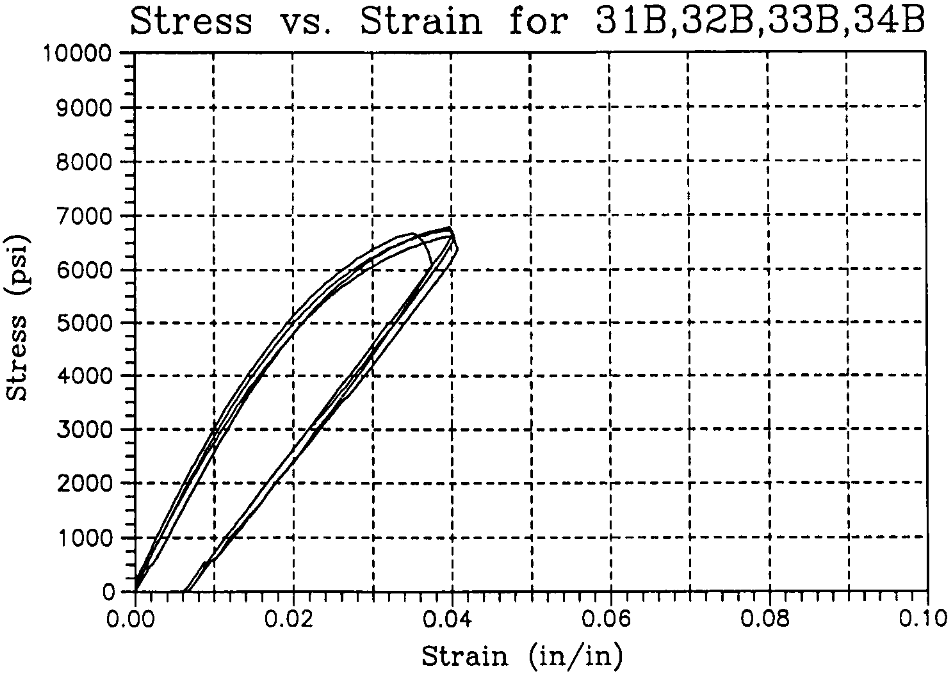

FIGURE 5 Loading/unloading diagram for experiment B, group 3 samples.

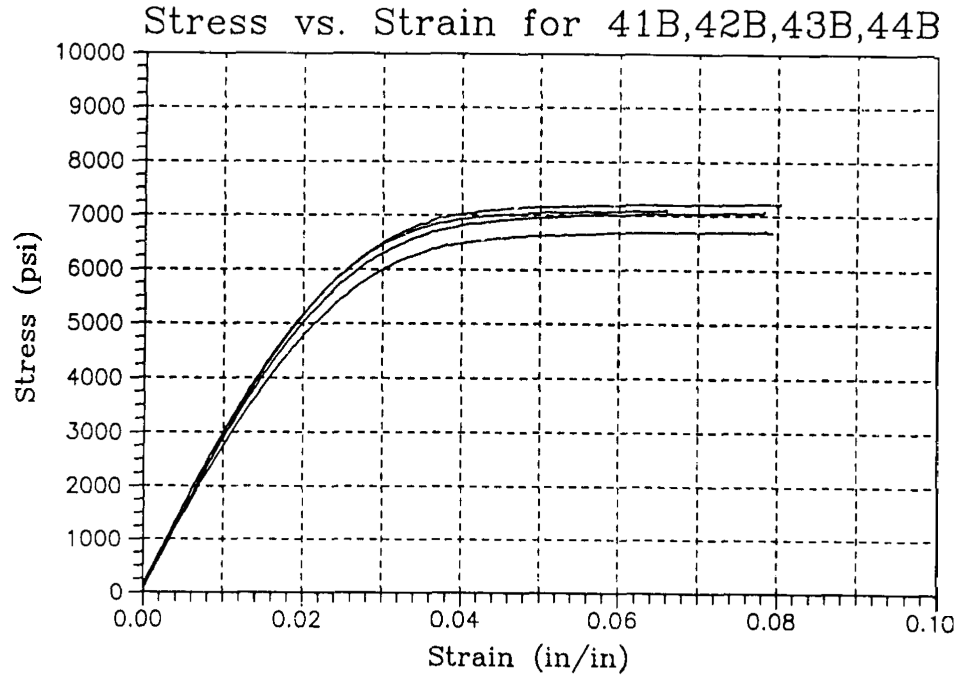

FIGURE 6 Loading diagram for experiment B, group 4 samples.

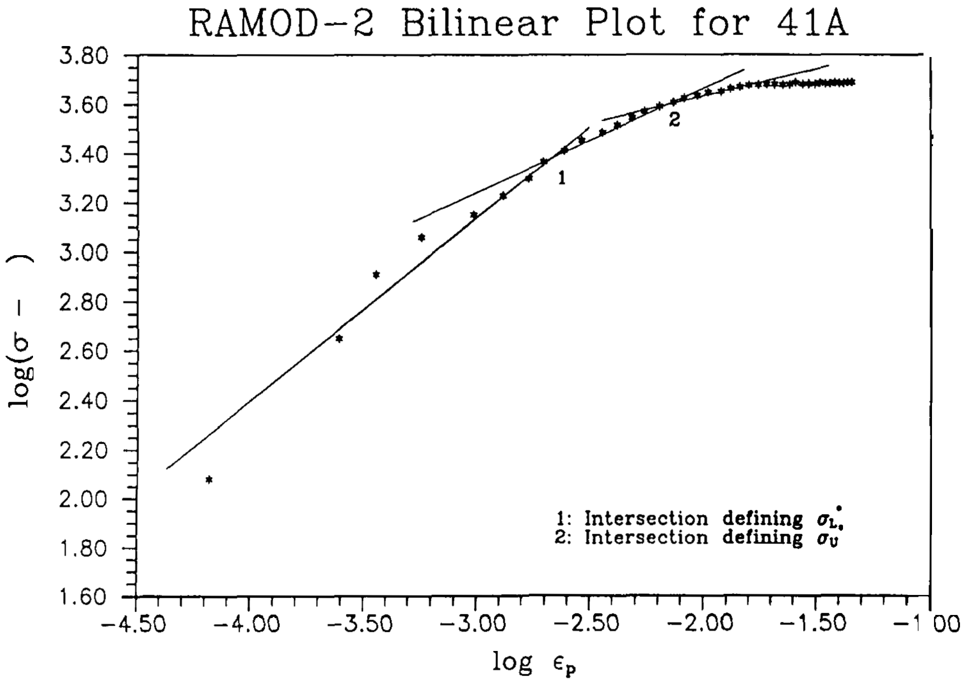

FIGURE 7 Sample RAMOD-2 plot illustrating the dual bilinear fit

TABLE I
Summary of loading and stress whitening data for experiment A

Sample No.	E (psi)	θ (psi)	σ_L^* (psi)	σ_U^* (psi)	σ_V^* (psi)
21A	310000	3600	—	—	—
22A	320000	3700	—	—	—
23A	325000	3400	—	—	—
24A	320000	3500	—	—	—
31A	335000	3500	5900	7390	—
32A	310000	3600	5840	7230	—
33A	315000	3250	5810	6970	—
34A	305000	3300	5590	6930	—
41A	330000	3500	5950	7480	8190
42A	330000	3325	5900	7400	7980
43A	340000	3200	6150	7370	7990
44A	330000	3600	6000	7400	8020

TABLE II
Summary of loading and stress whitening data for experiment B

Sample No.	E (psi)	θ (psi)	σ_L^* (psi)	σ_U^* (psi)	σ_V^* (psi)
21B	285000	3200	—	—	—
22B	275000	2900	—	—	—
23B	285000	2900	—	—	—
24B	280000	2950	—	—	—
31B	300000	3200	4610	5770	—
32B	270000	2950	4810	6110	—
33B	285000	3100	4650	6190	—
34B	280000	3000	4550	5880	—
41B	290000	3100	4550	5920	5980
42B	300000	3200	4680	5830	6170
43B	290000	3000	4780	5950	5960
44B	275000	2850	4630	5730	6150

All of the values discussed in this section can be reviewed in Tables I and II. Examination of these Tables reveals that all values for experiment B are lower than the values given for experiment A. The authors attribute this difference to approximately four months aging (at 0°F (−17.8°C)) of the adhesive material between the time group A and (subsequently) group B samples were cured and manufactured. The manufacturer of the film adhesive reports a limited shelf life of six months at 0°F (−17.8°C) and, although this time span was not exceeded, it is possible that the properties of the cured adhesive will decline depending on how far into this shelf life they were kept prior to curing.

Moisture Absorption Results

The absorption tests performed subsequent to stressing of the samples revealed a conclusive link between material damage (stress whitening) and moisture absorption. Reduced average absorption graphs[22] were used to determine and illustrate this link. These graphs consist of a plot of percent weight gain (p.w.g.) *versus* $(t)^{1/2}/L$ where t is absorption time and L is the thickness of the given coupon. The p.w.g. is simply a measure of the weight gained by the sample due to the absorbed moisture and was calculated as follows:

$$\text{p.w.g.}_t = (W_t - W_o)/W_o \tag{10}$$

where W_o is the initial dry weight of the coupon and W_t is the weight of the sample at time t.

While the actual weight of each coupon at each given time was recorded by hand, the average absorption data and the reduced absorption plots were computer generated. Two computer programs were written such that upon entering the recorded weights, times and thicknesses of each coupon, the programs would generate the data necessary to construct the respective plots.

The data obtained within each experiment were averaged by group. For example, the data obtained for the four samples in group 1 were averaged together at each measurement time. In this manner, only one curve was generated for the entire group of samples instead of four, one for each coupon. By following such a procedure any variances within the data would be smoothed out somewhat and any confusion which might have been caused by trying to plot and analyze sixteen curves for each experiment, instead of four, would be eliminated.

The reduced average absorption plots are shown in Figures 8 and 9 for experiments A and B respectively. According to the hypothesis which this work is trying to confirm, the moisture absorption plots and the reduced absorption plots should behave in the following manner. The group 4 samples in each experiment exhibited excessive stress whitening and, for reasons previously discussed, should therefore contain more internal free volume. Based on this, these samples should absorb a greater weight percentage of moisture at a faster rate than any of the other groups. The group 3 samples, which were only slightly stress whitened, should contain more free volume than the samples of groups 1 and 2, but less than the samples of group 4. Based on this, the plots of group 3 data should lie above the plots of groups 1 and 2 data but below group 4 curves. Finally, the group 2 samples were not stress whitened and should, therefore, contain virtually the same amount of internal free volume as the unstressed (group 1) samples. The plots of groups 1 and 2 data then, should parallel each other quite closely, while laying below the groups 3 and 4 curves.

Figures 8 and 9 reveal that the excessively-stress-whitened samples (groups 4) behaved as expected. They absorbed more moisture at a slightly faster rate than all of the other groups. This is demonstrated by the fact that in all of the graphs the group 4 curves lie above the other three curves.

In viewing the moisture absorption test results for experiment A (Figure 8) a slight irregularity can be seen around 300 $\text{hrs}^{1/2}/\text{in}$ (11.8 $\text{hrs}^{1/2}/\text{mm}$) in the reduced absorption plot. This irregularity was caused by a malfunction of the temperature bath control. Due to a power surge, and a subsequently blown fuse, the bath temperature dropped to room temperature (70°F (21°C)) and remained at this temperature for approximately ten days. Once the special fuse was replaced, the bath returned to its normal operating temperature (104°F (40°C)). The exact effect on experiment A due to this malfunction is unknown, but immediate reduction in the water concentration level due to the induced thermal contraction and the resulting reduction in free volume (see Equation 3) is clearly visible and is consistent with the theory presented. Due to the possibility of irreversible effects this malfunction may have caused, however, another absorption test was deemed necessary. Thus, experiment B was conducted.

As far as the behavior of group 4 data is concerned, the reduced average absorption plot for experiment B, shown in Figure 9, is quite similar to that for experiment A.

Figures 10 and 11 show data for groups 1 and 4 of experiment A with standard deviations for comparison purposes. Similar information for groups 3 and 4 of experiment B are provided in Figures 12 and 13.

In the reduced absorption plot for experiment A (Figure 8), the curve repre-

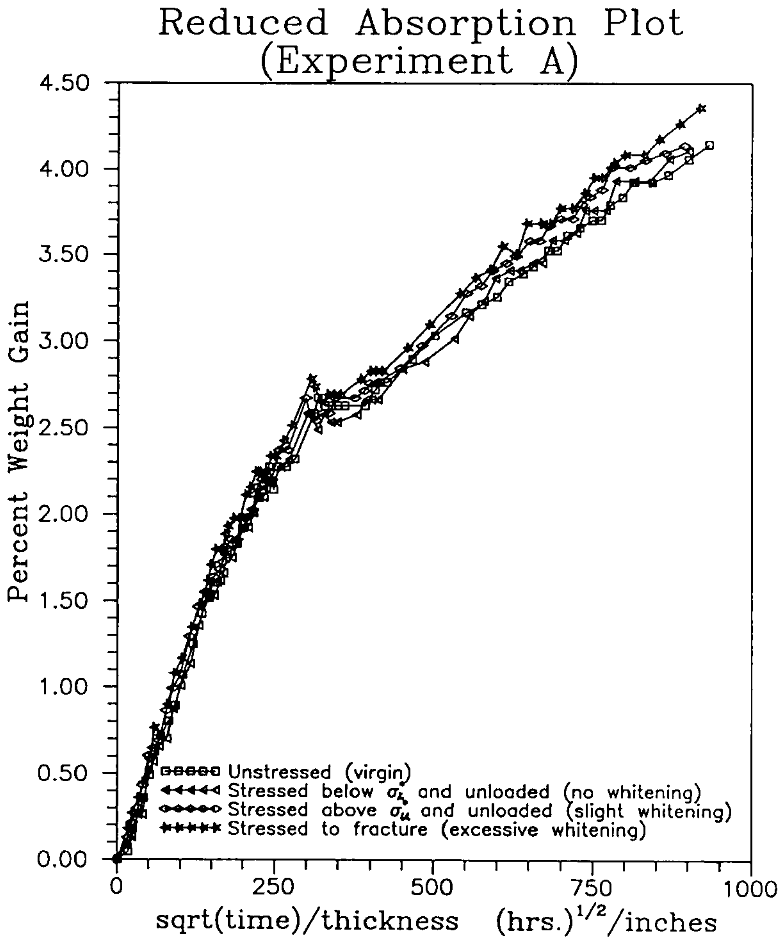

FIGURE 8 Reduced absorption plot for the samples of experiment A.

senting group 3A (slightly whitened samples) lies above the curves representing groups 1A and 2A and below the group 4A curve throughout virtually the entire time span. The group 1A and 2A curves also behaved as expected and parallel each other quite closely on both the average absorption and reduced absorption plots.

Approximation of the Bulk Moduli Ratio Based on Free Volume

We can calculate an approximate bulk moduli ratio K_f/K using equation (5). For this purpose, we will first assume that at the end of 2311 hours of immersion all the available free volume in the fractured samples of experiment B (group 4B) has been filled with water based on the shape of the reduced absorption plots shown in Figure 9. Based on this assumption, Figure 14 reveals that group 4 samples have an average 0.17 percent more free volume, f, than group 3 samples. Examination and compar-

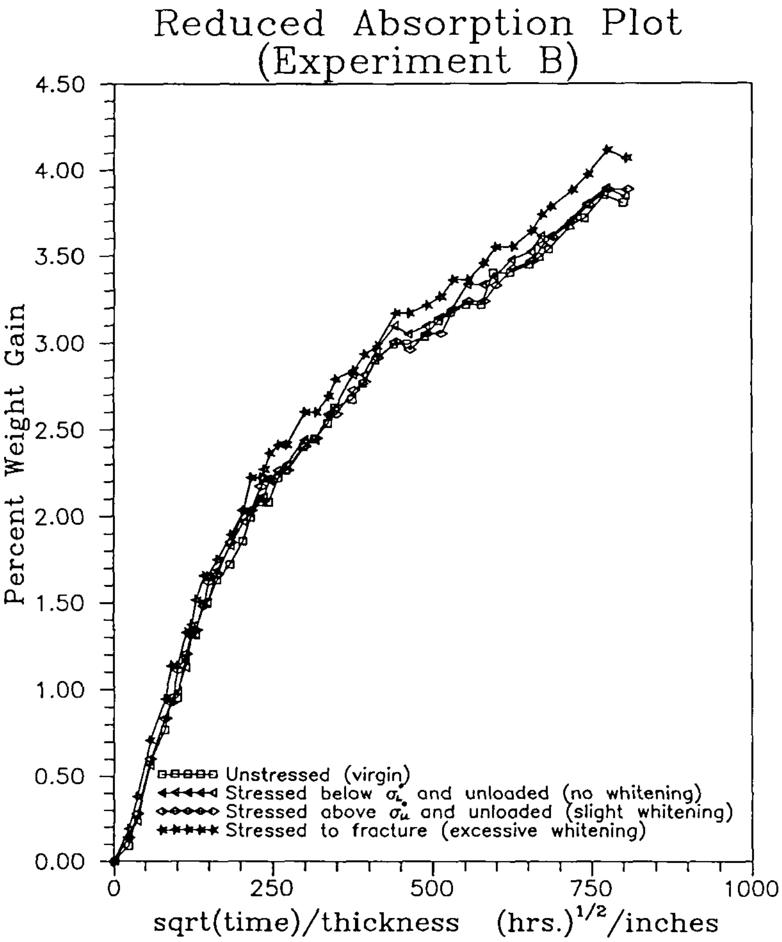

FIGURE 9 Reduced absorption plot for the samples of experiment B.

ison of Figures 5 and 6 reveal that group 4 samples have acquired approximately 3.4 percent more irreversible strain, ϵ_x, than group 3 samples. Finally, based on the results of Brinson *et al.*[6] for a comparable strain rate and adhesive material, we assume that the Poisson's ratio, ν, for the stress-whitened adhesive material is approximately 0.27. Substitution of these values in equation (5) results in an approximate bulk moduli ratio value of, $K_f/K = 9.2$. We note that this value should not be considered exact and it has been calculated only to illustrate its significant increase in the presence of stress whitening over the value $K_f/K = 2$ expected for non-stress-whitened materials.[17,23]

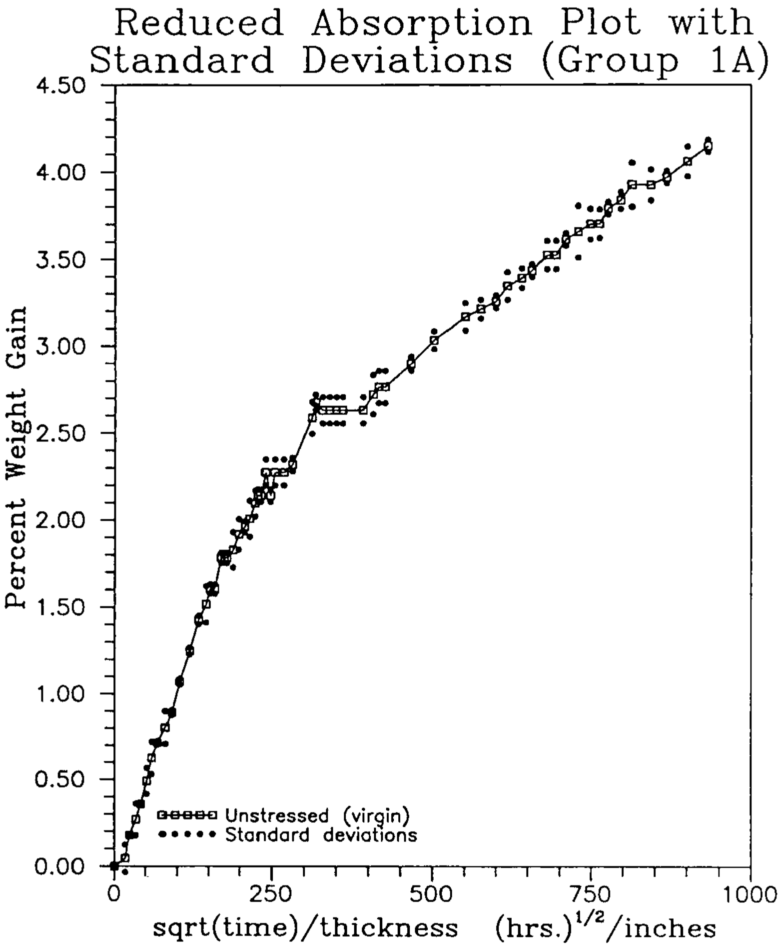

FIGURE 10 Reduced absorption plot for group 1A showing the standard deviation associated with each averaged data point.

CONCLUSIONS

Results of our experiments showed that samples which were excessively stress whitened as a result of fracture absorbed a greater weight percent of water than all other sample types. These excessively-stress-whitened samples also reached higher percentage weight gains in less time than other samples, indicating that the presence of stress whitening increases the rate of moisture absorption.

Unlike the frequently-reported procedure of water absorption under stress, our experiments were performed subsequent to loading/unloading or loading to frac-

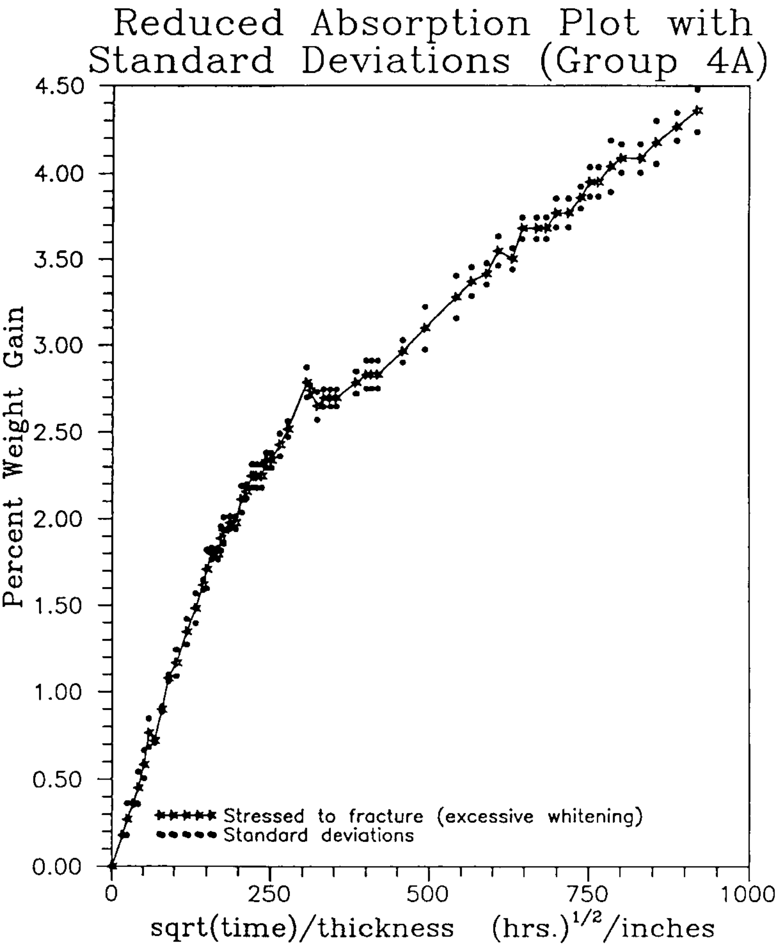

FIGURE 11 Reduced absorption plot for group 4A showing the standard deviation associated with each averaged data point.

ture. This was done to assess the effects of irreversible strains induced as a result of stress whitening and the ensuing increase in free volume. Indeed, the bulk moduli ratio, K_f/K, calculated based on our experimental measurements of irreversible strains and water absorption, is significantly higher than values reported in the literature.

We believe this result is significant in understanding the effects of water exposure on internal or external cracks present in an adhesive layer. In toughened epoxy adhesives the tip and path of cracks contain stress-whitened regions and such areas have now been shown to absorb more moisture in a shorter period of time in

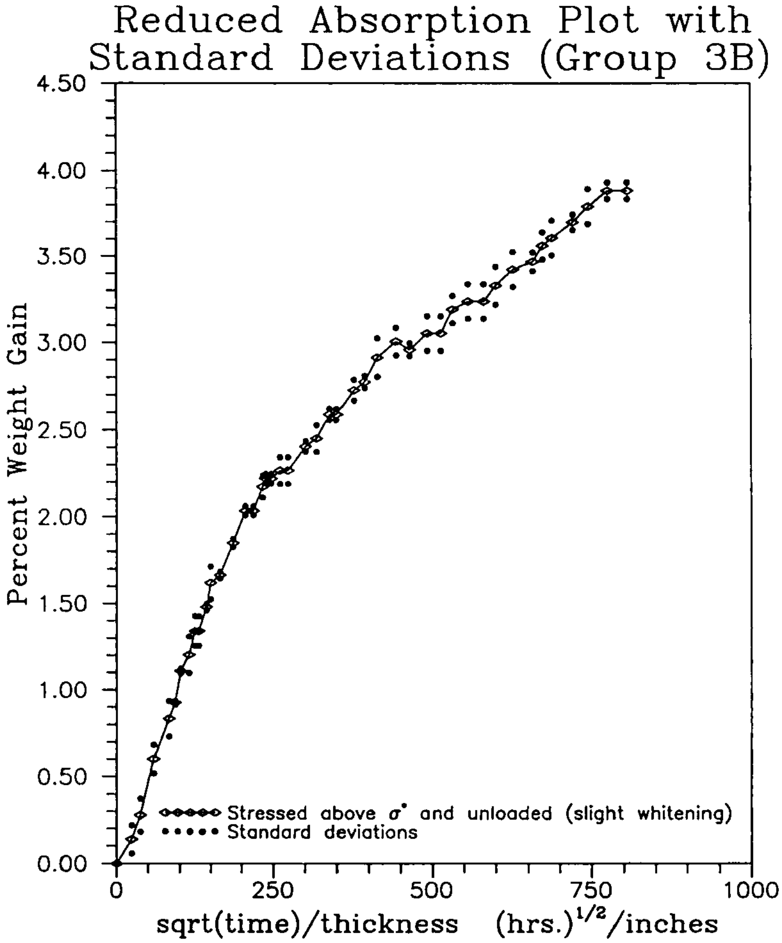

FIGURE 12 Reduced absorption plot for group 3B showing the standard deviation associated with each averaged data point.

comparison with the non-stress-whitened regions. Consequently, accelerated moisture effects may be expected in such areas and in their immediate neighborhoods due to deteriorating material properties and swelling. Furthermore, if crack propagation proceeds close to an interface the possibility of hydrolysis may increase again due to the accelerated moisture absorption shown. Such effects are usually studied with the use of a wedge test and the findings of this paper reveal the necessity to pay attention to the presence and location of stress whitening in interpreting the results of wedge tests performed in liquid or humid environments.

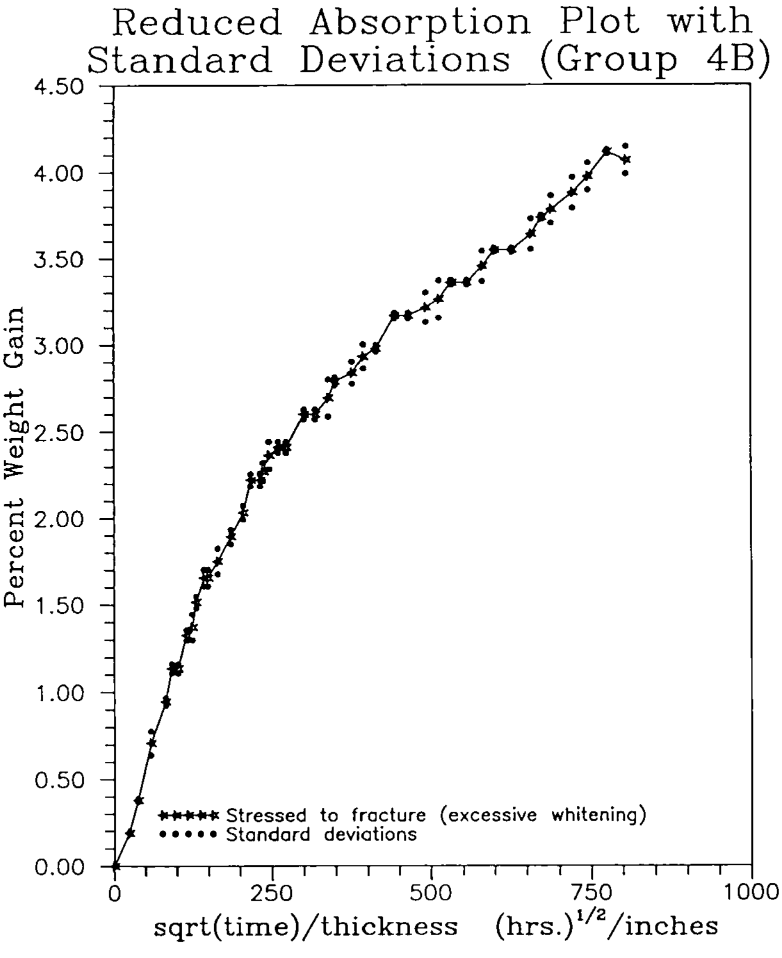

FIGURE 13 Reduced absorption plot for group 4B showing the standard deviation associated with each averaged data point.

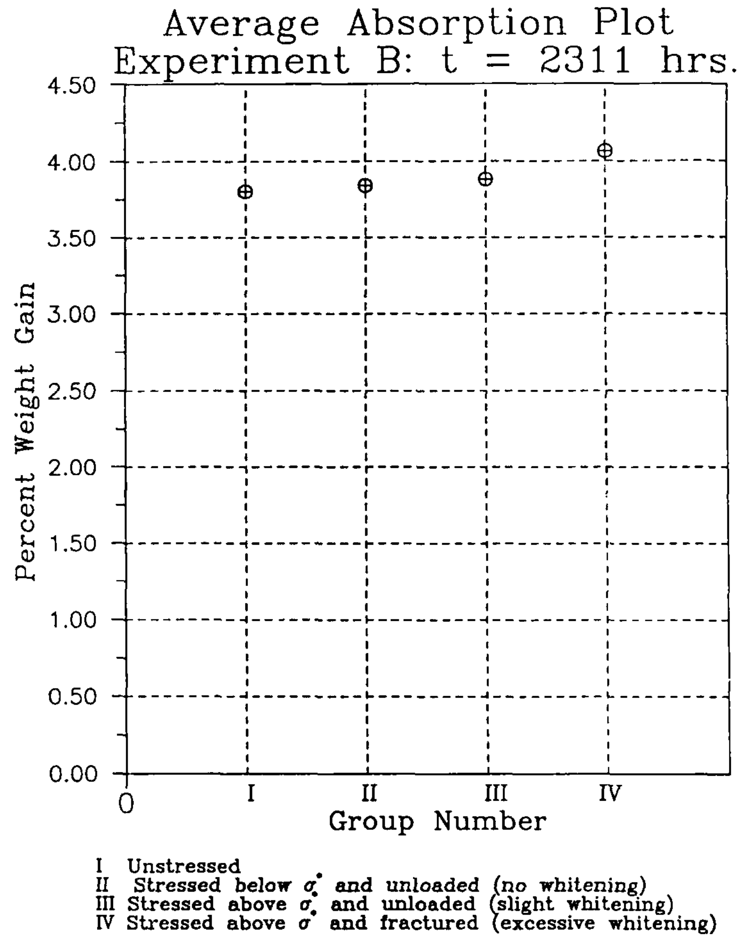

FIGURE 14 Experiment B average absorption data at t = 2311 hours.

References

1. R. G. Schmidt and J. P. Bell, *J. Adhesion* **25,** 85 (1988).
2. E. Sancaktar, H. Jozavi and R. M. Klein, *J. Adhesion* **15,** 241 (1983).
3. E. Sancaktar, *Experimental Techniques* **8,** 27 (1984).
4. H. Jozavi and E. Sancaktar, *J. Adhesion* **18,** 25 (1985).
5. E. Sancaktar, H. Jozavi, J. Baldwin and J. Tang, *J. Adhesion* **23,** 233 (1987).
6. H. F. Brinson, M. P. Renieri and C. T. Herakovich, **ASTM STP 593,** 177 (1975).
7. A. F. Yee and R. A. Pearson, *J. Material Sci.* **21,** 2462 (1986).
8. R. A. Pearson and A. F. Yee, *J. Material Sci.* **21,** 2475 (1986).
9. W. D. Bascom, R. L. Cottington and C. D. Timmons, *J. Appl. Polym. Sci.* **32,** 165 (1977).
10. D. L. Hunston, A. J. Kinloch, S. J. Shaw and S. S. Wang, in *Adhesive Joints: Formation, Characterization, and Testing,* K. L. Mittal, Ed. (Plenum Press, New York, 1982), p. 789.
11. G. R. Irwin, *Proc. Seventh Sagamore Conf. IV* p. 63 (1960).
12. D. Broek, *Elementary Engineering Fracture Mechanics* (Noordhoff International Publishing, Leyden, Netherlands, 1974), 3rd. edition.

13. J. W. Dally and R. J. Sanford, *Proc. of the 1985 Spring Conference on Experimental Mechanics*, p. 851 (1985).
14. H. Jozavi and E. Sancaktar, *J. Adhesion* **27,** 143 (1989).
15. H. Jozavi and E. Sancaktar, *J. Adhesion* **27,** 159 (1989).
16. D. R. Lefebvre, D. A. Dillard and T. C. Ward, *J. Adhesion* **27,** 1 (1989).
17. J. D. Ferry, *Viscoelastic Properties of Polymers,* (John Wiley & Sons Inc., New York, 1980), 3rd. edition, p. 292.
18. T. C. Wong and L. J. Broutman, *Polym. Eng. & Sci.* **25,** 521 (1985).
19. T. C. Wong and L. J. Broutman, *Polym. Eng. & Sci.* **25,** 529 (1985).
20. T. C. Wong, *Moisture Diffusion Mechanisms in Epoxy Resins,* Ph.D. Dissertation, Illinois Institute of Technology (1982).
21. M. P. Renieri, C. T. Herakovich and H. F. Brinson, "Rate and Time Dependent Behavior of Structural Adhesives," Virginia Polytechnic Institute and State University Report No: VPI-E-76-7 (1976).
22. J. Cromyn, in *Developments in Adhesives-2,* A. J. Kinloch, Ed. (Applied Science Publishers, London, 1981), p. 279.
23. S. Roy, D. R. Lefebvre, D. A. Dillard and J. N. Reddy, *J. Adhesion* **27,** 41 (1989).